

## X-RAY CAVITIES IN THE G50 BRIGHT GROUP-CENTERED GALAXY NGC 5846

Anil Kyadampure<sup>1</sup>, N. D. Vagshette<sup>2</sup> and M. K. Patil<sup>3</sup>

<sup>1</sup>*Department of Physics, Sanjeevane Mahavidyalaya, Chapoli Tq. Chakur Dist. Latur-413513, India*

<sup>2</sup>*Department of Physics and Electronics, Maharashtra Udayagiri Mahavidyalaya, Udgir,  
Dist. Latur-413517, India*

E-mail: [nilkanth1384@gmail.com](mailto:nilkanth1384@gmail.com)

<sup>3</sup>*School of Physical Sciences, Swami Ramanand Teerth Marathwada University, Nanded-431 606, India*

(Received: April 25, 2021; Accepted: June 7, 2021)

**SUMMARY:** We present results based on analysis of the currently available 29.86 ks *Chandra* data on the Bright Group-Centered Galaxy (BGG) NGC 5846 of G50 group. A pair of X-ray cavities have been detected within a radius  $\leq 1$  kpc along the North-East and South-West directions. The analysis yielded the average cavity energy, ages and mechanical power equal to  $\sim 3.1 \times 10^{48}$  erg,  $0.61 \times 10^7$  yr and,  $3.78 \times 10^{41}$  erg s<sup>-1</sup>, respectively. The luminosity of X-ray emitting gas within the cooling radius (20 kpc) was found to be  $2.4 \times 10^{41}$  erg s<sup>-1</sup>, in agreement with the mechanical cavity power. The ratio of radio luminosity to mechanical cavity power is found to be  $10^{-4}$ . The Bondi accretion rate of the central supermassive black hole (SMBH) is  $\sim 5.95 \times 10^{-5} M_{\odot} \text{ yr}^{-1}$  and the black-hole mass derived using the Bondi-accretion rate was found to be  $\sim 3.74 \times 10^8 M_{\odot}$ .

**Key words.** Galaxies: active – Galaxies: general – Galaxies: clusters: individual: NGC 5846 – Inter-galactic medium

### 1. INTRODUCTION

It is well established that feedback from active galactic nuclei (AGN) plays an important role in ejection of hot gas in an individual galaxy as well as galaxies in groups and clusters (Hoeft and Brüggem 2004, Dunn and Fabian 2006, McNamara and Nulsen 2007, Diehl and Statler 2008, David et al. 2009, Gastaldello et al. 2009, Sun et al. 2009, Dong et al. 2010). Recent high-resolution X-ray observations from *Chandra* and *XMM-Newton* Telescopes have shown that the X-ray emitting gas in the cores of cooling-flow galaxies does not cool directly from the plasma to the molecular phase, but rather it is

heated before condensing. The current most acceptable model is that the AGN residing at the core of the cluster dominant galaxy reheat the cooling X-ray gas through a more complicated feedback process (Soker and Pizzolato 2005). Further, *Chandra* and *XMM-Newton* observations have evidenced highly disturbed structures in the cores of several galaxy groups and clusters. These structures include cavities, shocks and sharp density discontinuities. Radio wavelength observations of such clusters have confirmed that the AGN jets emanating from central AGN yield such disturbances. Here, X-ray cavities are seen as depressions in the X-ray surface brightness filled with low density relativistic plasma and are a consequence of the displacement of thermal gas due to the AGN radio jets from central dominant galaxies (Fabian et al. 2003). Now it is widely accepted that mass accretion onto a central massive black hole is the ultimate source of energy for formation of such cavities. How-

---

© 2021 The Author(s). Published by Astronomical Observatory of Belgrade and Faculty of Mathematics, University of Belgrade. This open access article is distributed under CC BY-NC-ND 4.0 International licence.

ever, the intermediate details regarding the physical process involved in this complicated feedback mechanism need to be investigated. Further, X-ray cavities embedded in hot X-ray halos are useful in quantifying the energy injected into the intracluster medium (ICM) through the AGN activity. Currently available observing facilities at X-ray wavelengths with superb angular resolution have made it possible to detect such cavities or bubbles of a few to few tens of kpc size in galaxies, groups and clusters and have provided with the strongest observational evidences for the AGN feedback in galaxy clusters. X-ray observations with these telescopes and their systematic analysis of galaxies in groups and clusters have shown that about 20-25% of groups and clusters harbor such cavities and this detection rate may go even up to about 70-75% in the case of X-ray bright cool-core clusters (Dunn and Fabian 2006, Dong et al. 2010).

Majority of the systems hosting X-ray cavities are found to be associated with radio jets and spatially coincident with radio bubbles or lobes (McNamara and Nulsen 2007, Pellegrini et al. 2018, Bourne and Sijacki 2017). Combined X-ray and radio observations of X-ray cavities suggest that these cavities are usually inflated by bipolar jets emanating from the AGNs located at centres of such clusters (McNamara et al. 2009, Dong et al. 2010, Pandge et al. 2012, 2013, Sonkamble et al. 2015, Vagshette et al. 2016, 2017, 2019, Birzan et al. 2004, Rafferty et al. 2006). Further, it is observed that, like the extragalactic radio jets, X-ray cavities also appear in pairs (Wise et al. 2007, Pinto et al. 2018, Pasini et al. 2019) and are of ellipsoidal shapes. Majority of the X-ray cavities are filled with radio emission and some are connected to the nucleus of host galaxies through synchrotron jets and tunnels in the hot gas (Clarke et al. 2005). As the X-ray cavities are found to be driven outward by buoyancy forces, it is possible to estimate the dynamical age of these cavities by noting how far they are from the nucleus of the host galaxy. However, most of the studies of AGN feedback are confined to the AGN jets and cavity systems seen in the massive and X-ray luminous galaxy clusters, where the disturbed structures in the X-ray emission are clearly visible, while that in galaxies belonging to smaller groups have received less attention. In fact, most of the baryonic matter in the Universe reside in smaller groups and hence are the perfect laboratories to understand the impact of feedback on the formation and evolution of galaxies.

An earlier study of NGC 5846 by Machacek et al. (2011) detected a pair of cavities near nucleus and host cavities at 5.2 kpc. In this paper, we report a detailed analysis of *Chandra* X-ray data on NGC 5846, the brightest member of the G50 group with a focus on reinvestigating the morphological and temperature structure in the cavities and its effect on environment of the host galaxy. Moreover, we evaluate whether the mechanical energy generated by AGN is sufficient to balance radiation losses.

The structure of this paper is as follows. In Section 2 we shortly describe the observational data reduction procedure. The results of the study and discussions we provided in Section 3. Finally, the conclusion of this study is given in Section 4. We assume

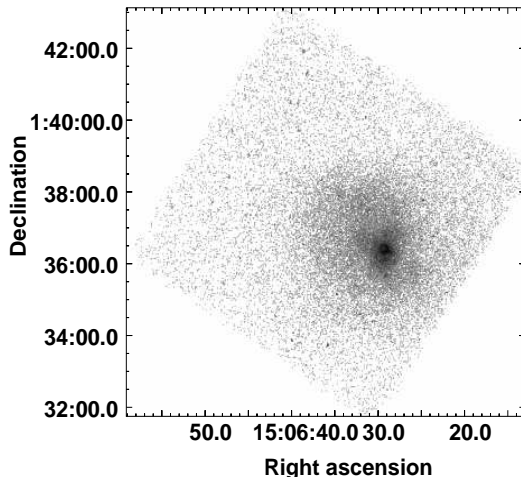


**Fig. 1:** Raw *Chandra* image of the full ACIS S3 chip ( $82 \times 82$  kpc) region of NGC 5846 in the 0.3 - 3.0 keV energy band. The X-ray emission is smoothly distributed in all direction.

$H_0 = 70 \text{ km s}^{-1} \text{ Mpc}^{-1}$ ,  $\Omega_M = 0.27$  and  $\Omega_\Lambda = 0.73$  translating to a scale of  $0.119 \text{ kpc arcsec}^{-1}$  at the redshift  $z=0.005717$  of NGC 5846. All spectral analysis errors are with 90% confidence, while all other errors are 68 % confident.

## 2. OBSERVATIONS AND DATA REDUCTION

NGC 5846, the brightest member of the G50 group, was observed by *Chandra* X-ray Observatory on May 24, 2000 by Dr. Ginevra Trinchieri for an effective exposure time of 29.86 ks (OBSID 788). The observations were carried out in the FAINT mode with the target centred on a back-illuminated chip ACIS-S3 and other chips in the switched-on mode (ACIS-235678). The X-ray data of NGC 5846 were retrieved from the *Chandra* Data Archive (CDA) and were reprocessed from the level-1 using the "chandra\_repro" routine provided by the *Chandra* Interactive Analysis of Observations (CIAO-4.2) and calibration files CALDB 4.1.2. For this we followed the standard *Chandra* data reduction threads<sup>1</sup>. Periods of high background flares were identified using the  $3\sigma$  clipping of light curve *lc\_sigma\_clip* and then they were binned in intervals of 200s. After removing these periods of high background count rates, the cleaned data have the net effective exposure time of 23.22 ks. The background subtraction was done by using the corresponding blank-sky event file. The light-curve in 2.5 - 7 keV was extracted from the blank-sky file and the observed flaring events were removed using the 'lc\_sigma\_clip' task of CHIPS package. The blank sky background subtraction was done by methods provided by Markevitch and Vikhlinin (2001).

<sup>1</sup><http://cxc.harvard.edu/ciao/threads/index.html>

**Table 1:** 1-D surface brightness profile.

Region	$\beta$	$r_c$ (")
Azumathal (0 – 360 deg.)	$0.42 \pm 0.002$	$7.21 \pm 0.25$
NE (0 – 180 deg.)	$0.37 \pm 0.004$	$5.56 \pm 0.55$
SW (180 – 240 deg.)	$0.47 \pm 0.010$	$14.90 \pm 1.30$

### 3. RESULTS AND DISCUSSION

#### 3.1. Surface Brightness Profile

The raw 0.3–3.0 keV *Chandra* image of NGC 5846 (Fig. 1) shows that the hot gas in the central region of this group is not distributed smoothly but instead shows fluctuations and discontinuities. These fluctuations in turn indicate the presence of large-scale gas motions or shocks in the hot gas surrounding the central bright galaxy NGC 5846. A surface brightness profile of the extended emission from NGC 5846 in 0.3 – 3.0 keV was derived by extracting counts from the concentric circular annuli to a radius of 140" from the center. Before that, all the point sources within chip were identified and removed. The left panel of Fig. 2 reveals that the X-ray emission in NGC 5846, like in the other cooling flow galaxies, shows a central peak which then declines outwards. At  $\sim 3''$  it shows a small excess in surface brightness which is perhaps due to the emission from filaments. Despite of the presence of X-ray cavities (depression) and other substructures, the azimuthally averaged surface brightness profile as a function of radial distance  $r$  for NGC 5846 exhibits smooth structure and, therefore, is fitted with the standard one-dimensional  $\beta$  model;

$$\Sigma(r) = \Sigma_0 \left[ 1 + \left( \frac{r}{r_c} \right)^2 \right]^{-3\beta+0.5},$$

where  $r_c$  represent the core radius. The best-fit parameters yielded by this analysis are  $r_c = 7''.21 \pm 0.25$  (0.86 kpc) and  $\beta = 0.42 \pm 0.002$ .

To highlight the depressions seen in the X-ray emission from cavity regions, we have generated (0.3 – 3.0) keV surface brightness profiles by extracting counts from two conical sectors namely, Sector 1 (covering the NE cavity) and Sector 2 (covering the SW cavity) from the background subtracted X-ray image. The angular coverage of these sectors (in west to north) are  $20^\circ$  to  $80^\circ$  and  $180^\circ$  to  $250^\circ$ , respectively. The resultant surface brightness profiles are shown in Fig. 2 (right panel), while the best fitted  $\beta$  model values are given in Table 1. Apart from the two main depressions, several other variations between about  $2''$  and  $20''$  for NE and at  $2''$  and  $50''$  for SW of the surface brightness profiles are evident (Fig. 2 right panel) and are perhaps representing the sloshing motions of hot gas in NGC 5846.

#### 3.2. X-ray cavities in NGC 5846

Presence of a pair of cavities in this galaxy has been already reported by Allen et al. (2006), Dong et al. (2010). However, to better visualize and verify these features we obtained residual images using *unsharp masking* and 2-D *elliptical  $\beta$ -model* subtraction (Dong et al. 2010). The background subtracted exposure corrected 0.3 – 5.0 keV image was used for this. In the unsharp-mask technique, a  $2\sigma$  ( $1\sigma = 0.5''$ ) Gaussian smoothed kernel image generated using *aconve* task was subtracted from a highly Gaussian smoothed ( $10\sigma$ ) image. The resultant residual image is shown in the left panel of Fig. 3. To confirm features seen in the unsharp map, we obtained a 2-D smooth image by fitting ellipses to the isophotes of X-ray image and fitted it with a 2-D beta model. The result of best fit beta models are the core radius  $r_c = 6''.11 \pm 0.5$  and  $\beta = 0.68 \pm 0.01$ . The resultant residual image produced after subtracting the beta model is shown in the right panel of Fig. 3. From both these images it is clearly evident that NGC5846 hosts a pair of depressions along the NE and SW direction and bright rims in the surface brightness distribution.

Further, to confirm these surface brightness depressions seen towards the NE and SW directions as cavities and their association with radio source, we used archival radio observation data. The 1.49 GHz radio frequency data on NGC 5846 from the VLA survey (NRAO/VLA Archive Survey) were used to derive a radio emission map to compare its association with X-ray features. The 1.49 GHz contours (black colour) generated from the emission map are overlaid on the smoothed X-ray (0.3 – 1.0 keV) image shown in the left panel of Fig. 4. From this figure it is clearly seen that the center of radio emission coincides with center of the X-ray source (blue cross represents central X-ray point source detected using the CIAO *wavdetect* task). The extent of radio emission from NGC 5846 matches well with the surface brightness depression seen in the residual X-ray image and hence confirms the presence of pair of X-ray cavities. The maximum extent of radio contours is  $\approx 3.68$  kpc along the NE-SW direction.

With a view to deduce the spectral properties of hot gas in cavities, filaments and other substructures in more detail, we have extracted X-ray spectra of emission from NE, SW-regions, the central  $2''$  region and the filamentary regions (N, S and W), shown in the right panel of Fig. 4. For the background treatment we extracted spectra using blank-sky background files. The source spectra were grouped to have at least 20 counts per bin to use  $\chi^2$  statistics. The spectral fitting was performed using X-Ray Spectral Fitting Package *XSPEC*. After an appropriate background subtraction each spectrum was fitted independently with an Astrophysical Plasma Emission Code (APEC) assuming collisionally ionized diffuse hot gas heated to temperatures of the order of  $(10 \text{ to } 100) \times 10^6$  K. This code uses atomic data to calculate spectral models for hot plasma along with the Galactic photoelectric absorption model *WABS*. The Hydrogen column density ( $n_H$ ) was kept fixed at the

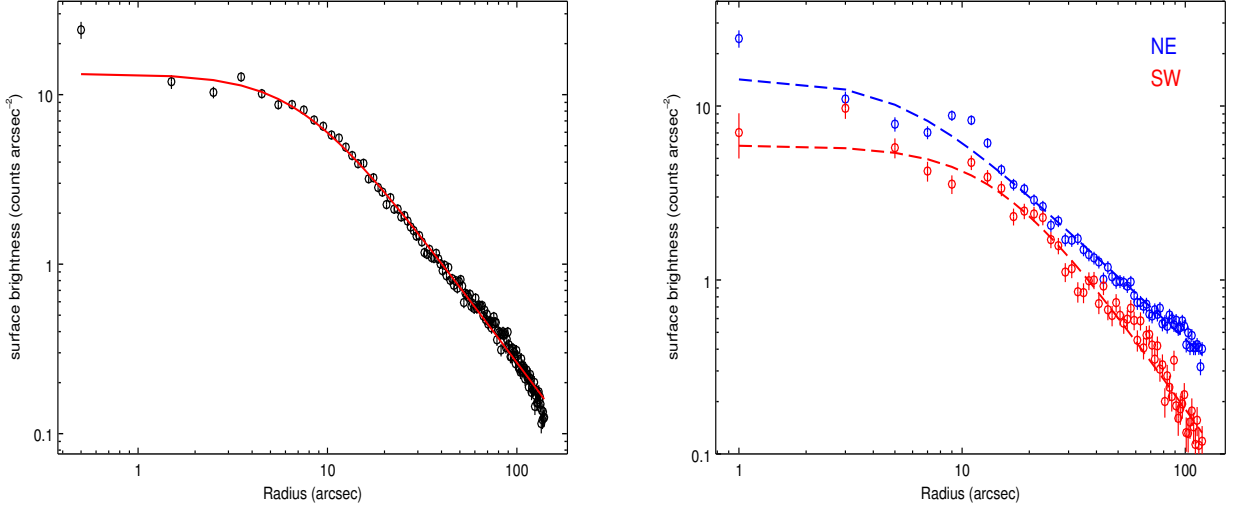


**Fig. 2:** *Left panel:* The azimuthally averaged, background subtracted 0.3 – 3.0 keV surface brightness profile of NGC 5846. The solid line represents the  $\beta$  model fit. *Right panel:* The background subtracted 0.3 – 3.0 keV surface brightness profiles of X-ray photons extracted from conical sectors covering NE ( $20^\circ$ -  $80^\circ$ , and SW ( $180^\circ$ -  $250^\circ$ ) cavities.

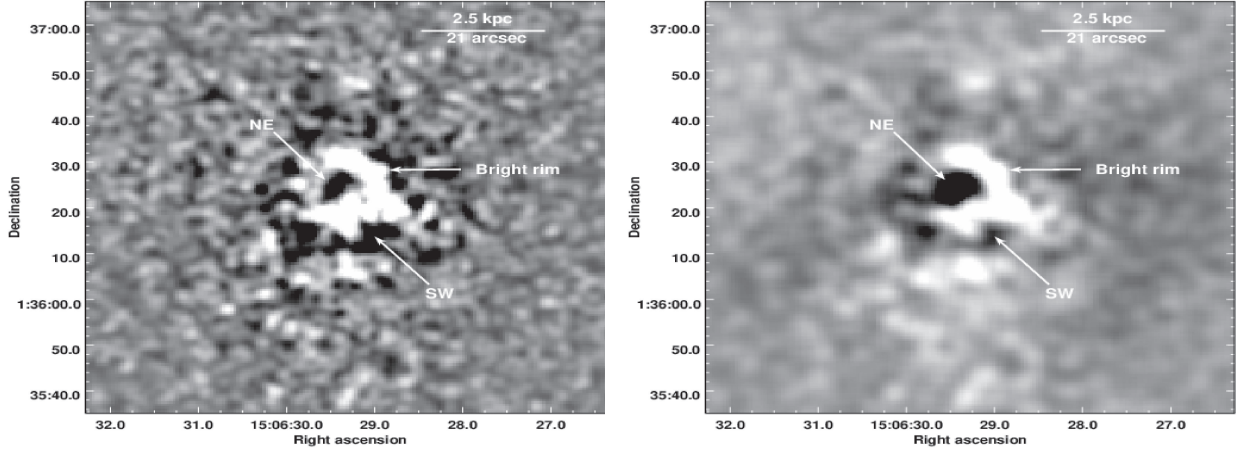


**Fig. 3:** *Left panel:* The unsharp-masked image of NGC 5846 in the energy band 0.3-3.0 keV produced by subtracting a  $2\sigma$  Gaussian kernel smoothed image from that smoothed with the  $10\sigma$  Gaussian kernel. *Right panel:* The ratio of 0.3 – 3.0 keV original image with the 2D- $\beta$  model image. Both these figures clearly reveal a pair of cavities (dark shades marked as NE and SW cavities) and filaments in the form of excess emission (white shades).

Galactic value equal to  $4.3 \times 10^{20} \text{ cm}^{-2}$ . All the spectra were fitted with  $WABS \times APEC$  unless and until not mentioned in the 0.5 – 5.0 keV energy band. The  $APEC$  code has four parameters, out of which, three parameters (temperature, abundance and normalization) were allowed to vary and redshift was frozen during the fit. The spectra extracted from the NE and SW cavities independently yielded temperature

values equal to  $0.72 \pm 0.04 \text{ keV}$  and  $0.63 \pm 0.052 \text{ keV}$ , respectively, while that from the N, S and W filaments resulted in to temperatures of  $0.70 \pm 0.04 \text{ keV}$ ,  $0.70 \pm 0.04 \text{ keV}$  and  $0.62 \pm 0.04 \text{ keV}$ , respectively. The temperature and metallicity values of hot gas in various regions are shown in Table 2. Throughout this paper the Chi-square goodness of fit was used during model fitting.

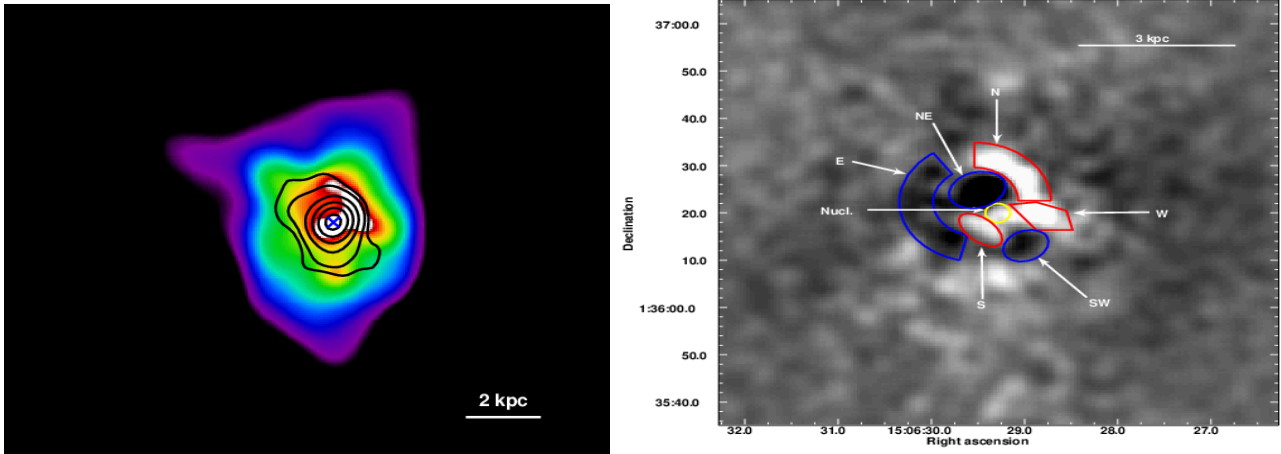


**Fig. 4:** *Left panel:* *Chandra* smoothed image (0.3-1.0 keV) of NGC 5846, overlaid with VLA 1.49 GHz contours. Blue cross shows the central X-ray point source. *Right panel:* This figure represents the regions of interest used for spectral extraction.

### 3.3. Cavity Energetics

With an objective to quantify the amount of energy injected by AGN into the ICM of NGC 5846 (cavity power) and to compare it with the energy lost by hot gas due to X-ray radiative process (i.e. gas luminosity inside the region occupied by the cavities) we measure the  $pV$  work done by the jet in inflating the cavity (McNamara and Nulsen 2007, Gitti et al. 2010). For this we measured the cavity enthalpy  $4pV$  (for relativistic plasma) and ages of cavities. The age of the cavity was estimated using three different ways: 1) assuming that the bubbles are rising with the local sound speed, 2) the bubbles are rising buoyantly at their terminal velocity and 3) the time required by the material to refill its volume as it rises outward (Birzan et al. 2004). The cavity age estimated from the sound crossing time  $t_{cs}$  (i.e. the time required for the cavity to rise the projected distance from the center of AGN to the observed location with the speed of sound) is:

$$t_{cs} = \frac{R}{v_{cs}} = R \sqrt{\mu m_H / \gamma kT},$$

where,  $R$  is the projected distance from the center of cavity to the center of AGN,  $v_{cs}$  is the speed of sound in that medium,  $\gamma = 5/3$ , and the mean molecular weight for ionised gas  $\mu = 0.62$ . Then, the total power of cavity was estimated as,

$$P_{cavity} = E_{total} / \langle t_{age} \rangle.$$

For comparison we also calculated the age of cavities by using the buoyancy time  $t_{buoy} \sim R \sqrt{2gV/S C_D}$ , where  $g \approx 2\sigma^2/R$  is the gravitational acceleration,  $S$  is the cross sectional area of cavity,  $V$  is the volume of cavity,  $\sigma$  is dispersion velocity and  $C_D = 0.75$  drag coefficient (Churazov et al. 2001). The refill time was

estimated as  $t_{ref} = 2\sqrt{r/g}$  where  $r$  is the equivalent radius of cavity ( $r = \sqrt{ab}$  where  $a$  and  $b$  are the semi-major and semi-minor axes of cavity, respectively). In the present case, the estimated age and power of cavities using all the three methods are reported in Table 3. From comparison of the three estimates it is clear that  $t_{buoy} < t_{cs} < t_r$ .

The total luminosity of gas inside the region occupied by the cavity was estimated as the bolometric X-ray luminosity,  $L_X$ , derived from the projection spectral analysis,  $L_X = 2.4 \times 10^{41} \text{ erg s}^{-1}$ . This indicates that the mechanical luminosity of the AGN outburst is large enough to balance the radiative losses. Radio observations at 1.4 GHz are useful to trace the AGN activities. NGC 5846 was detected at 1.4 GHz with flux density equal to 21.0 mJy (Filho et al. 2004), that corresponds to radio luminosity of  $2.11 \times 10^{37} \text{ erg s}^{-1}$ . The ratio of radio luminosity to power of the X-ray cavities is found to be  $\sim \times 10^{-4}$ , implying that the radio source is inefficient to carve these cavities.

### 3.4. Central Point Source

The central X-ray point source in NGC 5846 was found to be coincident with the radio nucleus (within  $0''.5$ ). To investigate its emission characteristics, we extracted the spectrum of this point source within the  $2''$  radius and fitted with wabs\*APEC model within XSPEC, which has 185 net counts in total band. The best-fit model yielded a  $kT = (0.63 \pm 0.08) \text{ keV}$  and flux  $2.0 \pm 0.26 \times 10^{-14} \text{ erg cm}^{-2} \text{ s}^{-1}$ , corresponding to luminosity of  $(1.50 \pm 0.20) \times 10^{39} \text{ erg s}^{-1}$ .

To calculate the accretion rate for SMBH, we used the Bondi (1952) model of steady, spherical, and adiabatic accretion. This needs the temperature and density at “infinity”, in practice near the accretion radius (i.e.  $r_A = GM_{BH}/c_s^2 \sim 9.14 \text{ pc}$ , where  $c_s$  is the sound speed and  $M_{BH}$  is the mass of SMBH sited in NGC 5846). Unfortunately, the spatial resolution

**Table 2:** Spectral parameters of cavities and other substructures of NGC 5846. The last column shows the goodness of fit (GOF).

Regions	Best-fit model	$kT$ (keV)	Abund. $Z_{\odot}$	GOF $\chi^2/\text{dof}$
NE-cavity	APEC	$0.72 \pm 0.05$	$0.48 \pm 0.05$	1.22
SW-cavity	APEC	$0.60 \pm 0.11$	$0.14 \pm 0.10$	0.98
N-structure	APEC	$0.70 \pm 0.04$	$0.51 \pm 0.04$	1.12
E-structure	APEC	$0.61 \pm 0.04$	$0.32 \pm 0.03$	0.72
S-structure	APEC	$0.70 \pm 0.04$	$0.33 \pm 0.04$	0.69
W-structure	APEC	$0.62 \pm 0.04$	$0.61 \pm 0.06$	0.82
Nucleus	APEC+APEC	$1.1 \pm 0.21$	$0.58 \pm 0.27$	0.60
		$0.50 \pm 0.08$	$0.42 \pm 0.08$	–

**Table 3:** Cavity properties of NGC5846.

Cavity Parameters	NE	SW
$a$ (kpc)	0.56	0.46
$b$ (kpc)	0.44	0.35
$R$ (kpc)	0.60	1.01
( $\text{cm}^{-3}$ )	$1.64 \times 10^{64}$	$9.34 \times 10^{63}$
$t_{cs}$ (yr)	$1.34 \times 10^7$	$0.25 \times 10^7$
$t_{\text{buoy}}$ (yr)	$0.98 \times 10^7$	$0.23 \times 10^7$
$t_{\text{refill}}$ (yr)	$2.86 \times 10^7$	$0.33 \times 10^7$
$P_{\text{cavity,cs}}$ ( $\text{erg s}^{-1}$ )	$4.31 \times 10^{41}$	$1.39 \times 10^{41}$
$P_{\text{cavity,buoy}}$ ( $\text{erg s}^{-1}$ )	$5.95 \times 10^{41}$	$1.48 \times 10^{41}$
$P_{\text{cavity,r}}$ ( $\text{erg s}^{-1}$ )	$2.02 \times 10^{41}$	$1.02 \times 10^{41}$

does not allow us to measure the temperature and density at this radius. However, these parameters at the accretion radius were estimated using the first-order polynomials for temperature and density profiles. We then estimated the Bondi accretion rate:

$$\dot{M}_{\text{Bondi}} = 8.4 \times 10^{21} M_8^2 T_{0.5}^{-3/2} n_1 \text{ g s}^{-1},$$

where  $M_8$  is the SMBH mass in the unit of  $10^8 M_{\odot}$  (for NGC 5846  $M_{\text{BH}} \simeq 3.47 \times 10^8 M_{\odot}$ , Ho et al. 2003),  $T_{0.5}$  is the temperature in the unit of 0.5 keV and  $n_1$  is the density in the unit of  $1 \text{ cm}^{-3}$  (see Baldi et al. 2009). The temperature and density at accretion radius are found to be 0.73 keV and  $0.23 \text{ cm}^{-3}$ , respectively. Using these values we estimate the Bondi accretion rate  $\dot{M}_{\text{Bondi}} \simeq 5.95 \times 10^{-5} M_{\odot} \text{ yr}^{-1}$ . At standard efficiency  $\eta \sim 0.1$ , as in brighter AGNs, it produces a luminosity:

$$L_{\text{acc}} = \eta \dot{M}_{\text{Bondi}} c^2 \simeq 3.36 \times 10^{41} \text{ erg s}^{-1},$$

This estimate is about 2 orders of magnitude higher than the observed luminosity, indicating the highly inefficient accretion scenario in NGC 5846.

#### 4. CONCLUSIONS

We have presented results based on the systematic analysis of 29.86 ks *Chandra* observations of a BGG NGC 5846 with an objective to study the properties of the X-ray cavities in its environment. Some of the important results from our analysis are summarized below:

1. The residual image derived from a 2-D beta model and unsharp masked image reveals presence of a pair of X-ray cavities in the central region of this system ( $\leq 1$  kpc) along the North-East and South-West directions.
2. The average energy content of the cavities, buoyancy age and total cavity power are found to be  $\sim 3.1 \times 10^{48}$  erg,  $0.61 \times 10^7$  yr and  $3.78 \times 10^{41}$   $\text{erg s}^{-1}$ , respectively.
3. Comparison of the cavity power with the cooling luminosity ( $\sim 2.4 \times 10^{41}$   $\text{erg s}^{-1}$ ) within the cooling radius reveals that the mechanical power injected by the AGN outburst is capable enough to compensate the radiative losses.
4. The ratio of radio luminosity to cavity power is  $\sim 10^{-4}$  implying that the radio source is inefficient to carve these cavities.
5. The Bondi accretion rate of central SMBH is found to be  $\sim 5.95 \times 10^{-5} M_{\odot} \text{ yr}^{-1}$  and the accretion luminosity derived from Bondi-accretion rate is  $\sim 3.36 \times 10^{41}$   $\text{erg s}^{-1}$ .

*Acknowledgements* – This work has made use of data from *CHANDRA* archive, NASA’s Astrophysics Data System(ADS), Extragalactic Database (NED). Radio contour used in this work are obtained from the NRAO/VLA survey. NDV thanks Science and Engineering Research Board (SERB), India for providing a research fund (Ref. No.: YSS/2015/001413). NDV also thanks IUCAA, Pune for the use of library facility.

## REFERENCES

- Allen, S. W., Dunn, R. J., Fabian, A. C., Taylor, G. B. and Reynolds, C. S. 2006, *BAAS*, **38**, 373
- Baldi, A., Forman, W., Jones, C., et al. 2009, *ApJ*, **707**, 1034
- Birzan, L., Rafferty, D. A., McNamara, B. R., Wise, M. W. and Nulsen, P. E. J. 2004, *ApJ*, **607**, 800
- Bondi, H. 1952, *MNRAS*, **112**, 195
- Bourne, M. A. and Sijacki, D. 2017, *MNRAS*, **472**, 4707
- Churazov, E., Brüggen, M., Kaiser, C. R., Böhringer, H. and Forman, W. 2001, *ApJ*, **554**, 261
- Clarke, T. E., Kassim, N., Ensslin, T. and Neumann, D. 2005, *Highlights of Astronomy*, **13**, 330
- David, L. P., Jones, C., Forman, W., et al. 2009, *ApJ*, **705**, 624
- Diehl, S. and Statler, T. S. 2008, *ApJ*, **687**, 986
- Dong, R., Rasmussen, J. and Mulchaey, J. S. 2010, *ApJ*, **712**, 883
- Dunn, R. J. H. and Fabian, A. C. 2006, *MNRAS*, **373**, 959
- Fabian, A. C., Sanders, J. S., Allen, S. W., et al. 2003, *MNRAS*, **344**, L43
- Filho, M. E., Fraternali, F., Markoff, S., et al. 2004, *A&A*, **418**, 429
- Gastaldello, F., Buote, D. A., Temi, P., et al. 2009, *ApJ*, **693**, 43
- Gitti, M., O’Sullivan, E., Giacintucci, S., et al. 2010, *ApJ*, **714**, 758
- Ho, L. C., Terashima, Y. and Okajima, T. 2003, *ApJ*, **587**, L35
- Hoefl, M. and Brüggen, M. 2004, *ApJ*, **617**, 896
- Machacek, M. E., Jerius, D., Kraft, R., et al. 2011, *ApJ*, **743**, 15
- Markevitch, M. and Vikhlinin, A. 2001, *ApJ*, **563**, 95
- McNamara, B. R. and Nulsen, P. E. J. 2007, *ARA&A*, **45**, 117
- McNamara, B. R., Kazemzadeh, F., Rafferty, D. A., et al. 2009, *ApJ*, **698**, 594
- Pandge, M. B., Vagshette, N. D., David, L. P. and Patil, M. K. 2012, *MNRAS*, **421**, 808
- Pandge, M. B., Vagshette, N. D., Sonkamble, S. S. and Patil, M. K. 2013, *Ap&SS*, **345**, 183
- Pasini, T., Gitti, M., Brighenti, F., et al. 2019, *ApJ*, **885**, 111
- Pellegrini, S., Ciotti, L., Negri, A. and Ostriker, J. P. 2018, *ApJ*, **856**, 115
- Pinto, C., Bambic, C. J., Sanders, J. S., et al. 2018, *MNRAS*, **480**, 4113
- Rafferty, D. A., McNamara, B. R., Nulsen, P. E. and Wise, M. W. 2006, in American Astronomical Society Meeting Abstracts, Vol. 209, American Astronomical Society Meeting Abstracts, 180.03
- Soker, N. and Pizzolato, F. 2005, *ApJ*, **622**, 847
- Sonkamble, S. S., Vagshette, N. D., Pawar, P. K. and Patil, M. K. 2015, *Ap&SS*, **359**, 21
- Sun, M., Voit, G. M., Donahue, M., et al. 2009, *ApJ*, **693**, 1142
- Vagshette, N. D., Sonkamble, S. S., Naik, S. and Patil, M. K. 2016, *MNRAS*, **461**, 1885
- Vagshette, N. D., Naik, S., Patil, M. K. and Sonkamble, S. S. 2017, *MNRAS*, **466**, 2054
- Vagshette, N. D., Naik, S. and Patil, M. K. 2019, *MNRAS*, **485**, 1981
- Wise, M. W., McNamara, B. R., Nulsen, P. E. J., Houck, J. C. and David, L. P. 2007, *ApJ*, **659**, 1153

**ШУПЉИНЕ У X-ЗРАЧЕЊУ NGC 5846, СЈАЈНОЈ  
ЦЕНТРАЛНОЈ ГАЛАКСИЈИ ГРУПЕ G50**

**Anil Kyadampure<sup>1</sup>, N. D. Vagshette<sup>2</sup> and M. K. Patil<sup>3</sup>**

<sup>1</sup>*Department of Physics, Sanjeevane Mahavidyalaya, Chapoli Tq. Chakur Dist. Latur-413513, India*

<sup>2</sup>*Department of Physics and Electronics, Maharashtra Udayagiri Mahavidyalaya, Udgir,  
Dist. Latur-413517, India*

E-mail: *nilkanth1384@gmail.com*

<sup>3</sup>*School of Physical Sciences, Swami Ramanand Teerth Marathwada University, Nanded-431 606, India*

УДК 524.7–735 NGC5846

*Оригинални научни рад*

Представљамо резултате засноване на анализи тренутно доступних посматрања телескопа Chandra, са експозицијом од 29.86 ks за сјајну централну галаксију групе G50, NGC 5846. Пар шупљина у X-зрачењу детектовано је унутар радијуса  $\leq 1$  крс, дуж правца север-исток и југ-запад. Анализом су добијене вредности средње енергије, старости и механичке снаге шупљина које износе  $\sim 3.1 \times$

$10^{48}$  erg,  $0.61 \times 10^7$  yr и  $3.78 \times 10^{41}$  erg s<sup>-1</sup>, респективно. Нашли смо да је луминозност гаса који зрачи у X-домену унутар радијуса хлађења (20 крс)  $2.4 \times 10^{41}$  erg s<sup>-1</sup>, у сагласности са механичком снагом шупљине. Бондијева стопа акреције за централну супермасивну црну рупу (СМЦР) је  $\sim 5.95 \times 10^{-5} M_{\odot}$  yr<sup>-1</sup>, а маса црне рупе изведена користећи Бондијеву стопу акреције износи  $\sim 3.74 \times 10^8 M_{\odot}$ .